Catalysis Science & Technology

Accepted Manuscript

ROYAL SOCIETY OF CHEMISTRY

www.rsc.org/catalysis

Journal Name

RSCPublishing

COMMUNICATION

Highly stable boron-modified hierarchical nanocrystalline ZSM-5 zeolite for methanol to propylene reaction†

Cite this: DOI: 10.1039/xoxxoooooox

Received ooth January 2012,
Accepted ooth January 2012

DOI: 10.1039/xoxxoooooox

www.rsc.org/

Zhijie Hu,‡ Hongbin Zhang,‡ Lei Wang, Hongxia Zhang, Yahong Zhang, Hualong Xu, Wei Shen* and Yi Tang*

A highly stable MTP catalyst of boron-modified hierarchical nanocrystalline ZSM-5 zeolite has been constructed by a facile salt-aided seed-induced route. Its cooperative effect of hierarchical structure and modified acidity gives rise to a significantly stable activity (725 h) even under a high WHSV of 4.0 h^{-1}.

With the increasing demands of propylene and the decreasing storage of petroleum resource in a post-oil society, the methanol to propylene (MTP) process has drawn significant attention in the chemical industry.[1] Over the last two decades, many fundamental researches have been conducted to develop effective catalysts with high selectivity and long lifetime for MTP.[2] Recent studies have demonstrated that ZSM-5 zeolite with a high Si/Al molar ratio is one of the most promising catalysts for MTP reaction owing to its characteristic MFI topology.[3] However, ZSM-5 zeolite still suffers from rapid/severe deactivation associated with carbon depositions during acid catalysed reaction process, which would result in covering the active sites or blocking the micropore channels of the catalyst, especially on the external surface.[4]

In order to solve the problem of rapid/severe deactivation and develop a highly stable catalyst for MTP, abundant new strategies have been proposed. In terms of pore structure design, hierarchical structured zeolite is an ideal alternative because it possesses the advantages of both mesoporous materials and zeolite crystals with well-improved mass transport properties.[5] Nanocrystalline[6] and nanosheet[7] ZSM-5 with short inner diffusion path have been adopted in several catalytic reactions to reduce the catalyst deactivation caused by pore blockage. Besides, the introduction of mesopores into the zeolite crystal during synthesis or post-synthesis modification, for examples by soft templating,[8] hard templating,[9] or alkaline treatment,[10] can also slow down the deactivation of the catalysts in MTP due to their improved mass transfer properties and tolerance for a larger amount of coke. The impacts of various mesopore types as well as hierarchical porosity in industrial catalysts have been evidently proven in the recent literatures.[11] On the other hand, the modification of acidity and addition of some active components also have been developed with some promising results. For example, phosphorus-modified ZSM-5 has been reported with improved catalytic stability and propylene selectivity.[12] On the approach of boron isomorphous substitution, it is found that the enhanced catalytic stability can be attributed to the increase of weak acid sites.[13] The introduction of gold nanoparticles into ZSM-5 can considerably stabilize the dehydrogenation intermediates during the coking process to reinforce the catalytic stability.[14] By the ways of either pore structure engineering or acidity modification, the lifetime of the catalysts can be prolonged from dozens to hundreds of hours at weight hourly space velocity (WHSV) of around 0.5-2.0 h^{-1}.[7-10, 12-14] However, from the point of practical view, the catalyst with longer lifetime even at higher WHSV is still desired especially via the preparation method with simple operations, high reproducibility and low energy-environment problems for large-scale production and industrial applications.[11, 15]

Herein, a highly stable MTP catalyst is designed by the combination of pore structure engineering and acidity modification. This catalyst of boron-modified hierarchical nanocrystalline ZSM-5 zeolite (denoted as B-N-Z5) displays the features of intercrystal mesoporosity from oriented self-assembled nano-crystallites and weak acidity of boron-modification. Based on the novel "salt-aided seed-induced route" recently proposed by our laboratory,[16] the one-step synthesis of B-N-Z5 catalyst shows the advantages of a fast crystallization process (within 4 h), high yield (>80%), low template consumption ($TPABr/SiO_2$ = 0.1) and no detectable extra-framework aluminum or boron species. Notably, an ultra-long lifetime (about 725 h) has been realized over this B-N-Z5 catalyst even under a high WHSV of 4.0 h^{-1}. Such an approach may bring new

possibilities for developing highly stable MTP reaction catalysts for industrial applications.

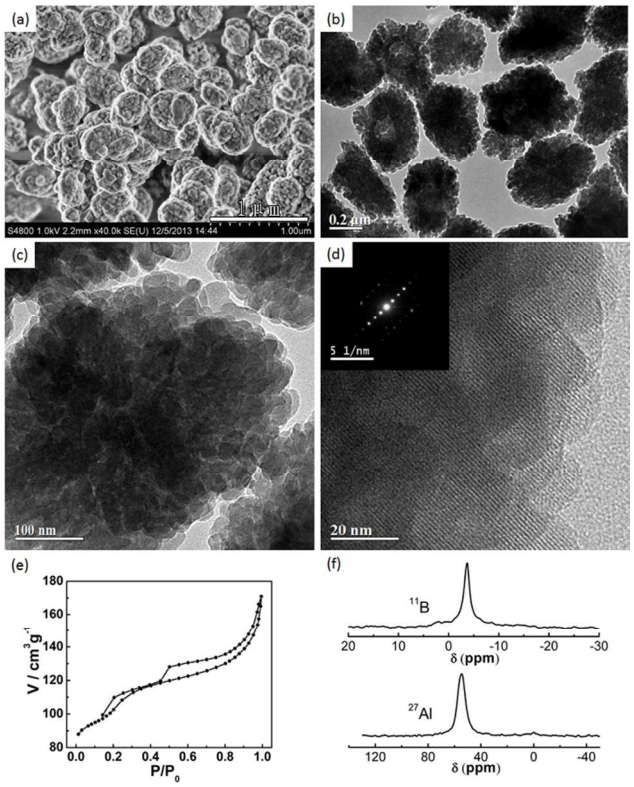

Fig. 1 (a) SEM, (b, c) TEM, (d) HRTEM and SAED images (inset of d), (e) N_2 sorption isotherm, (f) ^{11}B and ^{27}Al MAS NMR spectra of B-N-Z5.

The scanning electron microscopy (SEM) image is depicted in Fig. 1a. It clearly shows that B-N-Z5 sample exhibits a uniformly globular morphology with a diameter of about 500 nm and very rough external surface. The transmission electron microscopy (TEM) images of Fig. 1b and 1c show that each of the uniform zeolite microspheres is made up of abundant small nano-crystallite domains with an average diameter of about 20-40 nm. The in situ assembling of these nano-crystallites during the hydrothermal synthesis gives rise to abundant inter-crystallite mesopores amongst these zeolite nano-crystallites. High-resolution TEM (HRTEM) image in Fig. 1d further proves that these small nano-crystallites are highly crystalline and their lattice fringes exhibit the same orientation even extending over the whole zeolite aggregates, and the inset of selected area electron diffraction (SAED) presents a clear single-crystal-like diffraction pattern of ZSM-5 zeolite. This high-crystalline hierarchical nanocrystalline structure is also evidenced by the N_2 sorption isotherm (Fig. 1e), in which the B-N-Z5 sample shows a type IV isotherm with H3 hysteresis loop. The steep increase at low relative pressure ($P/P_0<0.2$) illustrates the perfect microporous structure in this sample while the special hysteresis loop appearing at P/P_0 = 0.1-0.4 is associated with the phenomenon of fluid-to-crystalline phase transition of adsorbed N_2 on the ZSM-5 zeolite with high Si/Al ratio.[17] Moreover, the B-N-Z5 has a large hysteresis loop and enhanced adsorption at intermediate and high pressures ($0.4<P/P_0<1$) arising from the nitrogen adsorption on inter-crystallite mesopores formed by the assembling of adjacent nano-crystallites, in agreement with the TEM image in Fig. 1c. In addition, the B-N-Z5 particles possess a highly mechanical stability, which are proved by the ultrasound experiment for 180 min after calcinations (Fig. S1).

The incorporation of B and its influence on the framework Al for B-N-Z5 are characterized by ^{11}B and ^{27}Al magic-angle-spinning nuclear magnetic resonance (MAS NMR) as shown in Fig. 1f. In the ^{11}B MAS NMR spectrum, an intensive and highly symmetric peak is observed at a chemical shift of ca. -3.9 ppm, which is characteristic peak of tetrahedral B species in the B-MFI framework.[18] And there is no peak at ca. –2.0 or above 5.0 ppm, which correspond to the extra-framework tetrahedral and the various trigonal B species respectively. In the ^{27}Al MAS NMR spectrum, there is only one peak at the chemical shift of ca. 55 ppm corresponding to the IV-coordinated Al in the framework. No signal at ca. 0 ppm, assigned to VI-coordinated extra-framework Al, is observed, indicating the Al species in this sample are all IV-coordinated framework Al. Therefore, the B species are completely incorporated into the B-N-Z5 zeolite framework and the existence of B does not affect the Al incorporation into the zeolite framework during the "salt-aided seed-induced route". The advantages of this method for heteroatom incorporation could also be proved by comparison with the conventional hydrothermal synthesis method reported in our previous work,[13] where not only extra-framework boron but also extra-framework aluminum species appeared (Fig. S2, †ESI).

Table 1 Compositions and textural properties of various samples

Sample	Si/Al[a]	B/Al[a]	S_L (m^2/g)	S_{ext}[b] (m^2/g)	V_{micro}[b] (cm^3/g)	V_{meso}[c] (cm^3/g)
C-Z5	156	0	435	52	0.12	0.07
N-Z5	152	0	489	122	0.11	0.19
B-C-Z5	160	0.58	452	67	0.12	0.07
B-N-Z5	162	0.62	460	109	0.11	0.18

[a] Determined by ICP-AES, [b] by *t*-plot method, [c] by *BJH* method. S_L: Langmair surface area; S_{ext}: external surface area; V_{micro}: micropore volume; V_{meso}: mesopore volume.

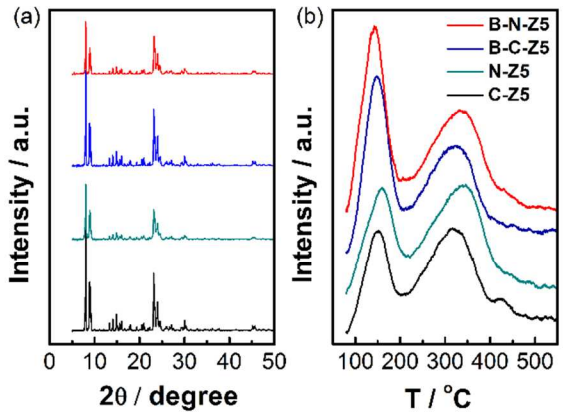

Fig.2 (a) XRD patterns and (b) NH_3-TPD profiles of C-Z5, N-Z5, B-C-Z5 and B-N-Z5

For more clearly investigating the effects of hierarchical structure and boron-modified acidity for B-N-Z5, a conventional ZSM-5 (denoted as C-Z5, Fig. S3a in †ESI, synthesized according to the Ref.[13]), a hierarchical nanocrystalline ZSM-5 (denoted as N-Z5, Fig. S4 in †ESI, synthesized according to the Ref.[16a]) and a B-modified conventional ZSM-5 (denoted as B-C-Z5, Fig. S3b and S5 in †ESI, the best catalyst with boron isomorphous substitution in the Ref.[13]) are adopted as the reference samples. Some detailed information on the C-Z5, N-Z5 and B-C-Z5 is described in †ESI. Their compositions and textural properties are summarized in Table 1. Elemental analysis by inductively coupled plasma-atomic emission spectrometry (ICP-AES) reveals that all these samples contain

similar Si/Al ratio of ca. 160. And B-C-Z5 and B-N-Z5 have the similar boron content. Moreover, all of the samples have large specific surface area (S_L, ca. 460 m^2g^{-1}) and microporous volume (V_{micro}, ca. 0.12 cm^3g^{-1}). The N-Z5 and B-N-Z5 possess much larger mesoporous volume (V_{meso}, ca. 0.19 cm^3g^{-1}) and external surface (S_{ext}, ca. 110 m^2g^{-1}) than C-Z5 and C-B-Z5 (ca. 0.07 cm^3g^{-1} and 60 m^2g^{-1}) due to their hierarchical nanocrystalline structure.

Fig. 2a depicts the powder X-ray diffraction (XRD) patterns of these four ZSM-5 samples. These samples all present the characteristic diffraction peaks for the typical structure of MFI topology at 2θ of 7.0-9.0 and 23.0-25.0, and no impure or amorphous phase is detected. However, the N-Z5 and B-N-Z5 samples present broader and weaker diffraction peaks, probably due to the submicron size of N-Z5 and B-N-Z5 particles. The acidities of the samples were characterized by temperature-programmed desorption of ammonia (NH_3-TPD). Fig. 2b displays the typical profile of zeolite with two desorption peaks, in which the peak at low temperature of around 150 °C (Peak I) is assigned to the weak acid sites while that at high temperature of around 330 °C (Peak II) is attributed to the strong acid sites. In detail, the strong acid amounts of these four samples are close to each other, in good agreement with their similar Si/Al ratio; while the weak acid amounts for B-C-Z5 and B-N-Z5 increase with the B incorporation into the ZSM-5 framework.[13] Besides, the Peak I of B-C-Z5 and B-N-Z5 display an interesting shift to lower temperature probably due to the weaker acidity of B-OH-Si;[13] while the Peak II of N-Z5 and B-N-Z5 have moved to a higher temperature probably due to the seed-induced synthesis method and the resulted special structure.[16a] This modified acidity by B incorporation is expected to exhibit improved catalytic performance in MTP reaction.

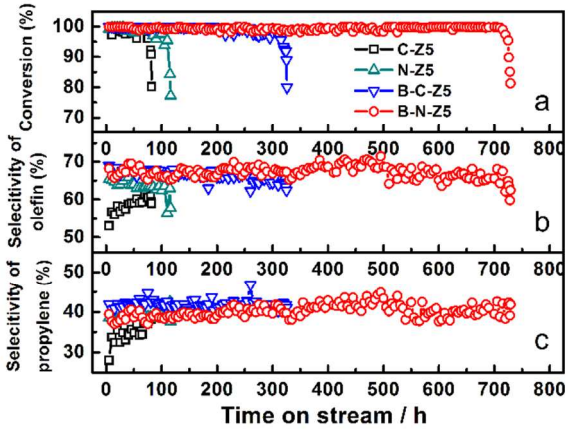

Fig. 3 Conversion of methanol (a), selectivity of total olefin (b) and propylene (c) over zeolites C-Z5 (Black), N-Z5 (Dark Cyan), B-C-Z5 (Blue) and B-N-Z5 (Red). *Reaction conditions*: WHSV = 4.0 h^{-1}, T = 733K, $n(CH_3OH) : n(H_2O) = 1 : 3$, P_{total} = 1 atm

To better study the catalytic stability of the B-N-Z5 for MTP reaction, the comparative tests were performed under approximate industrial condition (full methanol conversion)[6-15] but with a more harsh WHSV (4.0 h^{-1}, four times of the commonly used WHSV around 1.0 h^{-1} in literatures[6-10, 12, 14]) for accelerating the deactivation of catalysts. The results show that all the samples present a steady high methanol conversion of nearly 100% (Fig. 3a) and similar olefin and propylene selectivity (Fig. 3b and 3c). However, their activity would rapidly decay once the methanol conversions begin to reduce (Fig. 3a). The catalyst stability is estimated by using the reaction time for complete methanol conversion at a certain WHSV according to Ref.[6-15]. The B-N-Z5 catalyst displays the longest lifetime of 725 h (Fig. 3a) compared with C-Z5 of 80 h, N-Z5 of 120 h and even B-C-Z5 of 320 h. Referring to the textural and acidic properties shown above, the high stability of B-N-Z5 can be attributed to the cooperative effect of hierarchical structure and boron-modified acidity. In detail, compared with C-Z5 (80 h), the tendency of slowing-down deactivation of N-Z5 (120 h) is derived from its hierarchical nanocrystalline structure, which can shorten micropore channels to improve the diffusion property and accommodate more coke deposits.[6-7] The enhanced stability of B-C-Z5 (320 h) can be attributed to the increase of weak Brønsted acid sites by the B-incorporation. The introduction of more weak acid sites is believed to be able to speed up the reactions for olefin production and suppress the tendency for competitive polycyclic aromatization of the multi-methyl benzene intermediate to coke precursors.[13, 18-19] Combining the both advantages, the B-N-Z5 catalyst successfully realizes the cooperative effect of hierarchical structure and boron-modified acidity to the point, so that it performs a high stability for 725 h at a high WHSV of 4 h^{-1}, even much longer than the simple sum of those of N-Z5 with only hierarchical nanocrystalline structure (120 h) and B-C-Z5 with only boron modified acidity (320 h). Fig. S6 further displays the coke deposition at the deactivated catalysts measured by thermo-gravimetric (TG) analysis. It is found that the amount of coke follows the order of B-N-Z5 > B-C-Z5 > N-Z5 >> C-Z5, although the former has the highest stability. It indicates that the B-N-Z5 has a strong capability for coke tolerance due to the co-effect of the hierarchical porosity and unique acid distribution with enriched weak acid sites, which ensures the long-term maintenance of the catalytic activity until more coke is formed finally.

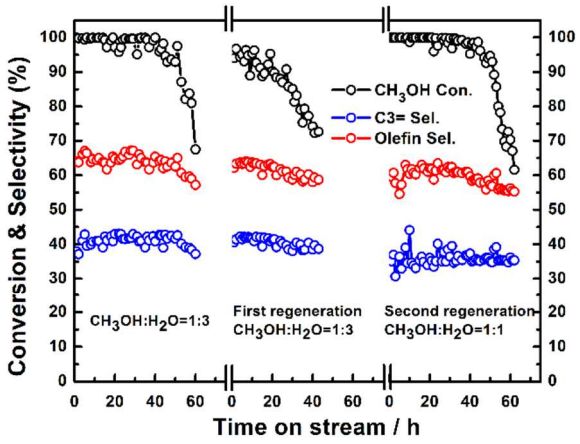

Fig. 4 Conversion of methanol, selectivity of total olefin and propylene over zeolite B-N-Z5. Reaction conditions: WHSV = 10 h^{-1}, T = 733 K, P_{total} = 1 atm. Regeneration conditions: in the air (40 $mLmin^{-1}$) atmosphere at 843 K for 8 hours.

The catalytic performance of B-N-Z5 has further been evaluated even at higher space velocity and with lower water content in the feed after several cycles of catalyst regeneration to deepen the understanding on the properties of B-modified hierarchical catalysts. As shown in Fig. 4, when the WHSV is increased to 10 h^{-1}, the B-N-Z5 still exhibits excellent performance with high methanol conversion (above 80%) after ca. 60 h with 65% olefin and 43% propylene selectivity. After regenerating the catalyst in the air (40 $mLmin^{-1}$) atmosphere at 843 K for 8 h, the B-N-Z5 still displays relative high methanol conversion (above 75%) after ca. 40 h at the

WHSV of 10 h^{-1}. In order to further study the catalyst stability, a third cycle has been carried out on the second regenerated catalyst at the WHSV of 10 h^{-1} and n(CH_3OH):n(H_2O) = 1:1. Interestingly, the B-N-Z5 shows high stability with high methanol conversion (above 80%) for 55 h under lower water ratio in the feed. To shed some light on the role of boron, a B/N-Z5 catalyst was prepared by impregnating similar amount of boron on N-Z5. The catalytic performance of B/N-Z5 was also evaluated at the WHSV of 10 h^{-1} (Fig. S7). The B/N-Z5 exhibits much shorter lifetime of only 9 h (methanol conversion above 80%) and lower olefin (< 60%) and propylene (34%) selectivity compared with B-N-Z5. Meanwhile, according to the XRD patterns (Fig. S8) of B/N-Z5 before and after the reaction, the appearance of alpha quartz was observed after only reaction of 12 h, probably due to its lower stability in steaming. However, the patterns of B-N-Z5 show almost no alteration. These results imply that the tetrahedral boron incorporated in the zeolite framework is important for the catalyst stability. The ^{11}B and ^{27}Al MAS NMR of B-N-Z5 after reaction were further employed to characterize the stability of the B and Al sites towards hydrolysis under the testing conditions. According to the results in Fig. S9, most of B and Al species are still IV-coordinated species in the framework although some defects or extra-framework species of B and Al are observed. Therefore, after the regeneration, the catalytic activity can still be maintained to some extent (Fig. 4) under the harsh reaction condition of WHSV = 10 h^{-1}.

Conclusions

In summary, boron-modified hierarchical nanocrystalline ZSM-5 zeolite (B-N-Z5) could be facilely prepared by a salt-aided seed-induced method, which provides the possibility for large-scale production due to the easy synthesis, fast crystallization and low usage of organic template. The systematic and thorough characterizations demonstrate that the typical B-N-Z5 catalyst not only has rough external surface, abundant intercrystal mesopores and high crystallinity, but also possesses increasing amount of weak acid sites arising from the framework incorporation of boron. And this B-N-Z5 catalyst shows a very long lifetime of 725 h even under the condition of high WHSV of 4.0 h^{-1} for the MTP reaction, which could be attributed to the unique cooperative effect of hierarchical nanocrystalline structure and boron-modified acidity in this sample. The results shown here indicate the necessity of combination of pore structure design and acidity modification for the highly stable MTP catalyst.

This work was supported by National Key Basic Research Program of China (2013CB934101), and Science and Technology Commission of Shanghai Municipality (11JC1400400).

Notes and references

Department of Chemistry, Shanghai Key Laboratory of Molecular Catalysis and Innovative Materials, Laboratory of Advanced Materials, and Collaborative Innovation Center of Chemistry for Energy Materials, Fudan University, Shanghai 200433 (P.R. China).

E-mail: yitang@fudan.edu.cn (YT), wshen@fudan.edu.cn (WS);

Fax: (+86) 21-65641740

† Electronic Supplementary Information (ESI) available: [synthesis procedure, characterization method, catalyst test, SEM and TEM images, ^{11}B and ^{27}Al MAS NMR spectra, TG curves, catalytic performance on MTP, XRD patterns]. See DOI: 10.1039/c000000x/

‡ The authors contributed equally to this work.

1. a)U. Olsbye, S. Svelle, M. Bjorgen, P. Beato, T. V. W. Janssens, F. Joensen, S. Bordiga and K. P. Lillerud, *Angew Chem Int Edit*, 2012, **51**, 5810-5831; b)M. Stocker, *Micropor Mesopor Mat*, 1999, **29**, 3-48; c)D. Lesthaeghe, A. Horre, M. Waroquier, G. B. Marin and V. Van Speybroeck, *Chem-Eur J*, 2009, **15**, 10803-10808; d)U. Olsbye, M. Bjorgen, S. Svelle, K. P. Lillerud and S. Kolboe, *Catal Today*, 2005, **106**, 108-111; e)Z. M. Cui, Q. Liu, W. G. Song and L. J. Wan, *Angew Chem Int Edit*, 2006, **45**, 6512-6515; f)W. Wang, Y. J. Jiang and M. Hunger, *Catal Today*, 2006, **113**, 102-114; g)W. Wang, A. Buchholz, M. Seiler and M. Hunger, *J Am Chem Soc*, 2003, **125**, 15260-15267.
2. a)Q. Zhu, J. N. Kondo, T. Tatsumi, S. Inagaki, R. Ohnuma, Y. Kubota, Y. Shimodaira, H. Kobayashi and K. Domen, *J Phys Chem C*, 2007, **111**, 5409-5415; b)A. T. Aguayo, A. G. Gayubo, R. Vivanco, M. Olazar and J. Bilbao, *Appl Catal a-Gen*, 2005, **283**, 197-207; c)B. P. C. Hereijgers, F. Bleken, M. H. Nilsen, S. Svelle, K. P. Lillerud, M. Bjorgen, B. M. Weckhuysen and U. Olsbye, *J Catal*, 2009, **264**, 77-87; d)M. Bjorgen, S. Svelle, F. Joensen, J. Nerlov, S. Kolboe, F. Bonino, L. Palumbo, S. Bordiga and U. Olsbye, *J Catal*, 2007, **249**, 195-207; e)S. Ilias and A. Bhan, *Acs Catal*, 2013, **3**, 18-31.
3. a)J. F. Haw, W. G. Song, D. M. Marcus and J. B. Nicholas, *Accounts Chem Res*, 2003, **36**, 317-326; b)J. Z. Li, Y. X. Wei, G. Y. Liu, Y. Qi, P. Tian, B. Li, Y. L. He and Z. M. Liu, *Catal Today*, 2011, **171**, 221-228; c)A. G. Gayubo, A. T. Aguayo, M. Olazar, R. Vivanco and J. Bilbao, *Chem Eng Sci*, 2003, **58**, 5239-5249.
4. H. Schulz, *Catal Today*, 2010, **154**, 183-194.
5. a)L. H. Chen, X. Y. Li, J. C. Rooke, Y. H. Zhang, X. Y. Yang, Y. Tang, F. S. Xiao and B. L. Su, *J Mater Chem*, 2012, **22**, 17381-17403; b)J. Perez-Ramirez, C. H. Christensen, K. Egeblad, C. H. Christensen and J. C. Groen, *Chem Soc Rev*, 2008, **37**, 2530-2542.
6. M. Firoozi, M. Baghalha and M. Asadi, *Catal Commun*, 2009, **10**, 1582-1585.
7. a)M. Choi, K. Na, J. Kim, Y. Sakamoto, O. Terasaki and R. Ryoo, *Nature*, 2009, **461**, 246-U120; b)S. Hu, J. Shan, Q. Zhang, Y. Wang, Y. S. Liu, Y. J. Gong, Z. J. Wu and T. Dou, *Appl Catal a-Gen*, 2012, **445**, 215-220.
8. J. Kim, M. Choi and R. Ryoo, *J Catal*, 2010, **269**, 219-228.
9. C. Sun, J. M. Du, J. Liu, Y. S. Yang, N. Ren, W. Shen, H. L. Xu and Y. Tang, *Chem Commun*, 2010, **46**, 2671-2673.
10. a)C. S. Mei, P. Y. Wen, Z. C. Liu, H. X. Liu, Y. D. Wang, W. M. Yang, Z. K. Xie, W. M. Hua and Z. Gao, *J Catal*, 2008, **258**, 243-249; b)P. N. R. Vennestrom, M. Grill, M. Kustova, K. Egeblad, L. F. Lundegaard, F. Joensen, C. H. Christensen and P. Beato, *Catal Today*, 2011, **168**, 71-79.
11. a)M. Milina, S. Mitchell, P. Crivelli, D. Cooke and J. Pérez-Ramírez, *Nat Commun*, 2014, **3922**, doi:10.1038/ncomms4922; b)S. Mitchell, N. L. Michels, K. Kunze and J. Perez-Ramirez, *Nat Chem*, 2012, **4**, 825-831.
12. J. Liu, C. X. Zhang, Z. H. Shen, W. M. Hua, Y. Tang, W. Shen, Y. H. Yue and H. L. Xu, *Catal Commun*, 2009, **10**, 1506-1509.
13. Y. S. Yang, C. Sun, J. M. Du, Y. H. Yue, W. M. Hua, C. L. Zhang, W. Shen and H. L. Xu, *Catal Commun*, 2012, **24**, 44-47.
14. C. Sun, Y. S. Yang, J. M. Du, F. Qin, Z. P. Liu, W. Shen, H. L. Xu and Y. Tang, *Chem Commun*, 2012, **48**, 5787-5789.
15. R. Chal, C. Gerardin, M. Bulut and S. van Donk, *Chemcatchem*, 2011, **3**, 67-81.
16. a)H. B. Zhang, Y. C. Ma, K. S. Song, Y. H. Zhang and Y. Tang, *J Catal*, 2013, **302**, 115-125; b)H. B. Zhang, K. S. Song, L. Wang, H. X. Zhang, Y. H. Zhang and Y. Tang, *Chemcatchem*, 2013, **5**, 2874-2878.
17. J. C. Groen, L. A. A. Peffer and J. Pérez-Ramírez, *Micropor Mesopor Mat*, 2003, **60**, 1-17.
18. R. Millini, G. Perego and G. Bellussi, *Top Catal*, 1999, **9**, 13-34.
19. a)Q. J. Zhu, J. N. Kondo, T. Yokoi, T. Setoyama, M. Yamaguchi, T. Takewaki, K. Domen and T. Tatsumi, *Phys Chem Chem Phys*, 2011, **13**, 14598-14605; b)Q. J. Zhu, J. N. Kondo, T. Setoyama, M. Yamaguchi, K. Domen and T.

Tatsumi, *Chem Commun*, 2008, 5164-5166; c)E. Unneberg and S. Kolboe, *Appl Catal a-Gen*, 1995, **124**, 345-354; d)M. Guisnet, L. Costa and F. R. Ribeiro, *J Mol Catal a-Chem*, 2009, **305**, 69-83; e)D. Mores, J. Kornatowski, U. Olsbye and B. M. Weckhuysen, *Chem-Eur J*, 2011, **17**, 2874-2884.